Numerical experiments with a model of a supercritical geothermal system

John O'Sullivan, Mike O'Sullivan, Adrian Croucher, Jeremy Riffault, Michael Gravatt and Ryan Tonkin

Department of Engineering Science and Biomedical Engineering, The University of Auckland, Private bag 1142, Auckland, New Zealand

jp.osullivan@auckland.ac.nz

Keywords: *Supercritical geothermal system, numerical model.*

ABSTRACT

We have set up a numerical model of a supercritical geothermal system and used it to carry out numerical experiments on the natural state of the system and its response to various production/injection scenarios. The model is based on a synthetic geothermal system that we use in teaching various courses on geothermal modelling, but we have extended the area of the model considerably and deepened it to ~ 8km. Thus, the model is large enough to act as a whole-of-system model and includes a supercritical zone at depth. In the experiments on the natural state model, we investigate what permeabilities are required at depth to allow the formation of a supercritical zone. In the experiments on the production scenarios, we investigate deep and mid-depth production and deep and mid-depth injection giving four possible scenarios.

1. INTRODUCTION

1.1 Background

The drilling of the deep wells IDDP-1 and IDDP-2 in Iceland has stimulated worldwide interest in supercritical geothermal resources (Elders et al. 2014; Dobson et al., 2017; Reinsch et al., 2017), particularly in Iceland (Fridleifsson, 2017; Scott, 2018;), Japan (Tsuchiya, 2017; Asunamu *et al.*, 2019, 2021; Ishitsuka *et al*., 2021; Suzuki *et al*., 2022; Oka et al., 2023) and New Zealand (Carson, 2018; Climo *et al*., 2020; Carey *et al*., 2021; Rendel *et al*., 2021;) but also in other countries (Stimac *et al*., 2017; Driesner, 2021; Feng *et al*., 2021a,b; Lamy-Chappuis, 2021, 2023; Wang *et al*., 2022).

Recently, there has been much discussion of "superhot" geothermal systems (e.g., Cladouhos & Callahan, 2024). They are systems with a high enthalpy but may have pressures below the critical point for water (220.64 bar) and, in this case, are not supercritical.

A recent article (Gunnarsson et al., 2024) discusses the production/injection options for developing a superhot/supercritical geothermal resource. In the present study, we use modelling to investigate options like these using a synthetic model based on geothermal fields in the Taupo volcanic zone (TVZ), New Zealand.

1.2 Supercritical simulators

The U.S. Geological Survey simulator HYDROTHERM (Hayba and Ingebritsen, 1994) was the first to have supercritical capability. This was followed by the HOTH2O extension to the STAR simulator (Pritchett, 1995) and the development of a supercritical equation of state (EOS) (Kissling, 1995) for MULKOM, the predecessor of TOUGH2 (Pruess *et al*., 1999). Kissling (2014) later developed a new supercritical simulator called TGNS.

The development of a supercritical equation of state, EOS1sc, for TOUGH2 was reported by Brikowski (2001), but its application has not been further discussed.

Croucher & O'Sullivan (2008) developed a new version of EOS1sc for the simulator AUTOUGH2, employing the updated IAPWS-97 thermodynamic properties of water (Wagner *et al*., 1997). O'Sullivan *et al*. (2020) modified EOS1sc to improve the phase changes near the critical point. This final version of EOS1sc has been incorporated into the iTOUGH2 framework (Magnusdottir & Finsterle, 2015; Magnusdottir & Jonsson, 2018).

In parallel, Xu and co-workers developed an alternative version of EOS1sc for TOUGH2 (Xu et al., 2020) and extended the capability of TOUGHREACT to cover supercritical conditions (Feng et al., 2021ab; Xu et al., 2023).

Driesner et al. (2015) developed a new simulator with supercritical capability known as the Complex Systems Modeling Platform (CSMP++). It has THMC options. i.e., it includes mechanical effects and chemical changes as well as thermal and hydraulic modelling. For example, it can handle H_2O-NaCl mixtures (Weis et al., 2014).

1.3 Previous models of supercritical geothermal systems

Much of the supercritical geothermal modelling to date has been generic, e.g., looking at convection above a cooling magma body (Hayba & Ingebritsen, 1987; Magnusdottir, 2014; Scott et al., 2015a,b, 2016, 2018; Andersen &Weis, 2020), and the brittle-ductile transition (Kissling et al., 2010; Afanasyev, 2020; Scott et al., 2024)

Several studies of production from idealized supercritical geothermal reservoirs have been carried out. For example, Yano & Ishido (1998) used a 2D radially symmetric model (R-Z) to investigate short and long-term behaviour and Sudamardi et al. (2012) used a 2D vertical slice model of the natural state followed by production simulations.

Parisio et al. (2019) used a THM model, implemented in finite element solver Open-GeoSys, to investigate the long-term risks of reinjection into supercritical geothermal systems.

Simulations of doublet injection/production, triplets or five-spot arrangements in supercritical geothermal reservoirs have been carried out by Watanabe et al. (2000), Brikowski (2001), Croucher & O'Sullivan (2008), Pashkevich & Taskin (2010).

The drilling of the deep wells, IDDP-1 and IDDP-2, reaching supercritical conditions at Reykjanes, Iceland, have provided data for several modelling studies, e.g., Scott et al. (2015b), Battistelli et al. (2018, 2020), Renaud et al. (2019), Hermanska et al. (2019), and Lamy-Chappuis et al. (2021, 2023).

ISSN 2703-4275

Kissling and co-workers have carried out several supercritical modelling studies of generic models of the Taupo volcanic zone, New Zealand, aimed at unravelling its structure and understanding the nature of the heat sources (Kissling, 1996, 1997, 1998, 1999; Kissling et al., 2009, 2010; Ellis et al., 2015). The studies by Kissling & Ellis (2011, 2012) included THM effects by coupling the SULEC thermo-mechanical code (Ellis et al., 2011) with a supercritical version of TOUGH2 (Kissling, 1995).

There have also been a few supercritical modelling studies of real geothermal fields (see Table 1).

Table 1: Supercritical modelling studies of real geothermal fields

Field	Reference
Simple 3D model of the deep seated reservoir at Kakkonda, Japan	Sato et al., 2000, 2003
3D model of Menengai, Kenya	O'Sullivan et al., 2015
2D model of Basse Terre Island in Guadeloupe	Raguenel et al. 2019
3D models of Menengai, Krafla, Reykjanes Peninsula and the Taupo volcanic zone	O'Sullivan et al., 2020
3D model of the Reykjanes Peninsula, Iceland	Barton & O'Sullivan, 2021
3D models (coarse and fine) of Krafla, Iceland	Scott et al., 2022
2D model of the Taupo volcanic zone, New Zealand	Kissling et al., 2024

2. SYNTHETIC MODEL

2.1 Standard Teaching Model

The standard model (Renaud *et al*., 2021) was set up for a synthetic, but representative geothermal reservoir on which to demonstrate the modelling process. The geology for the synthetic geothermal system was generated by GNS Science, based on existing New Zealand geothermal fields and typical geothermal formations. In summary, the geological context corresponds to a representative geothermal system with volcanic formations, with sedimentary surface deposits intercalated and intersected by three faults. Deep upflows at temperatures of up to 270°C create a geothermal system. Figure 1 shows a 3D representation of the conceptual model, including the low conductivity clay cap. The deepest formation is defined as a basement and is covered, in ascending order up to the surface, with ignimbrite, rhyolite, sediments, andesite, dacite, alluvium and superficial deposits.

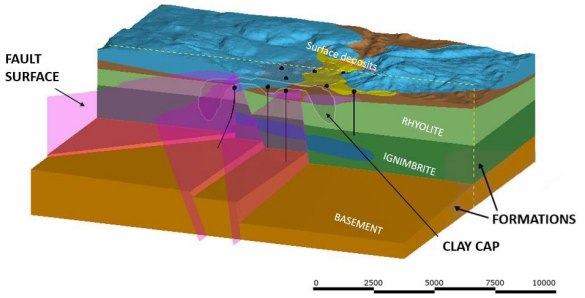

Figure 1: 3D representation of the conceptual model of the synthetic system, showing a faulted high temperature volcanic geothermal reservoir.

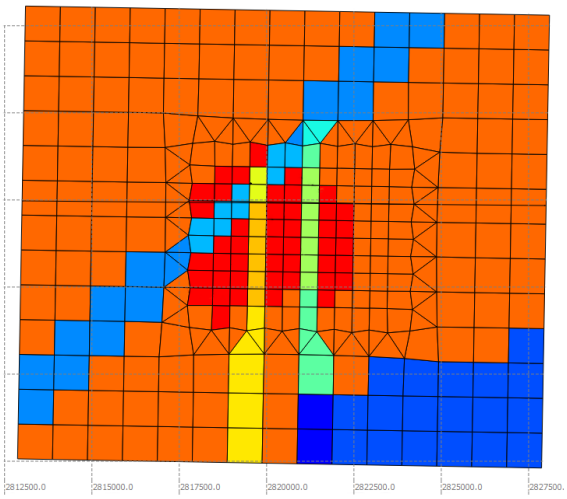

Figure 2: Rock-type distribution at the bottom layer of the model (layer 69).

Figure 2 presents a layer of the model grid, which has a total of 11764 blocks and covers an area of 13 km × 15 km. The three faults shown in Figure 1 are defined separately using their own dedicated rock-types. The grid is refined in the central area where the wells are located, as displayed in Figure 2.

The model has 69 layers and extends down to an elevation of -3500 m from mountainous terrain with an elevation varying from 80 m up to 880 m. In simulations with the standard teaching model, an air/water equation of state is used, and an unsaturated vadose zone is present at higher elevations.

It is assumed that 8 wells have been drilled, with downhole temperature profiles available that can be used to calibrate a natural state model.

2.2 Enlarged Teaching Model

To turn the teaching model into a supercritical system, we enlarged the area and made it much deeper. The enlarged teaching model has an area of 21 km x 23 km (4 km added on each side) and extends down to an elevation of -7750 m (8 extra layers, each 500 m thick). The permeability structure of the standard model was embedded without change in the enlarged model, and the permeability of the new blocks at the sides and in the deep zone was adjusted to create a system with a supercritical zone. The faults were assumed to extend laterally and with depth. A plot of vertical permeability in the new layer 69 is shown in Figure 3.

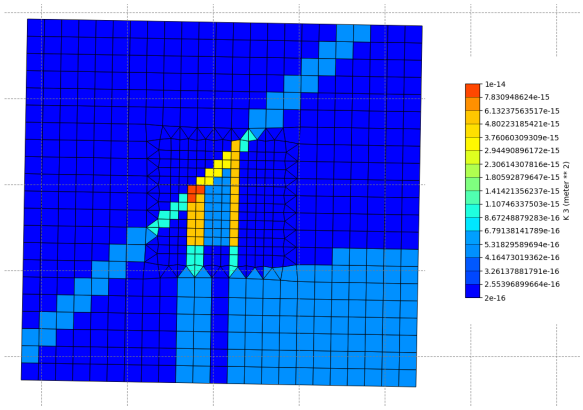

Figure 3: Vertical permeability distribution in layer 69 of the enlarged model.

The heat flux boundary conditions set at the base of the model are shown in Figure 4. This distribution was designed to create a convective geothermal system with supercritical conditions near the base and a reasonably hot geothermal system at 2-3 km depth, with no input of magmatic fluid.

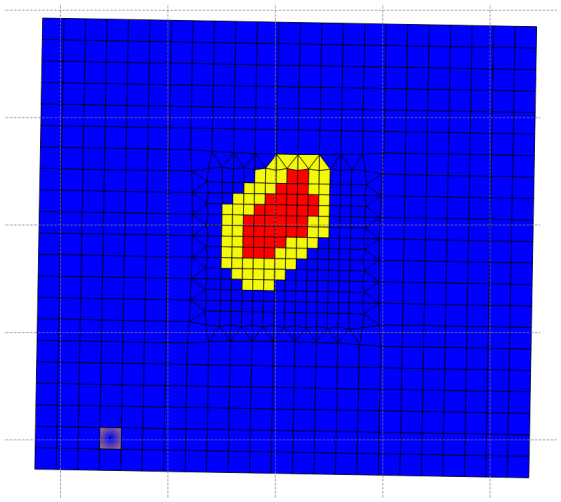

Figure 4: Heat flux at the base of the model: blue 0.1 W/m^2, yellow 2.4 W/m^2, red 3.84 W/m^2.

The corresponding temperature in the bottom layer is shown in Figure 5 and a vertical slice is shown in Figure 6.

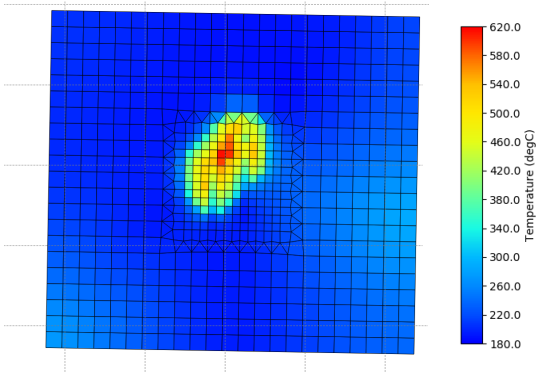

Figure 5: Temperature distribution on the bottom layer of the model.

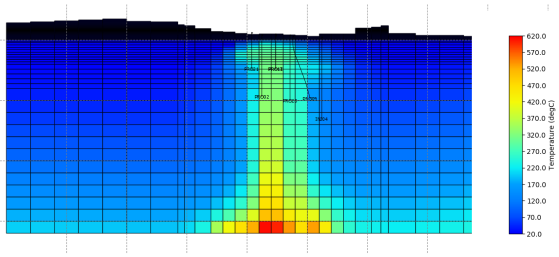

Figure 6: Temperatures on a W-E slice through the hottest part of the model. Some wells are shown for later reference.

The temperature distribution on the inner part of the model for layer 67 (elevation -2250 mRL) is shown in Figure 7. It shows that the convective plume is still hot (maximum temperature is ~ 325°C) at this elevation but is not supercritical. The locations of production wells (PRO30), injection wells (INJ40, INJ41) and one monitor well (WEL05) are shown.

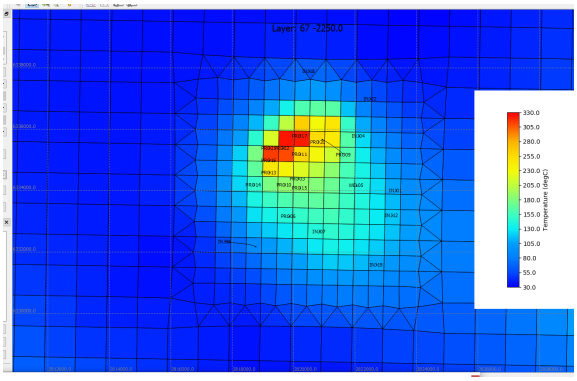

Figure 7: Temperature distribution on the inner part of the model for layer 67 (elevation -2250 mRL).

There are 134 blocks in the model with a temperature greater than 370°C. These are shown in Figure 8 on a plot of pressure vs temperature (including enthalpy contours).

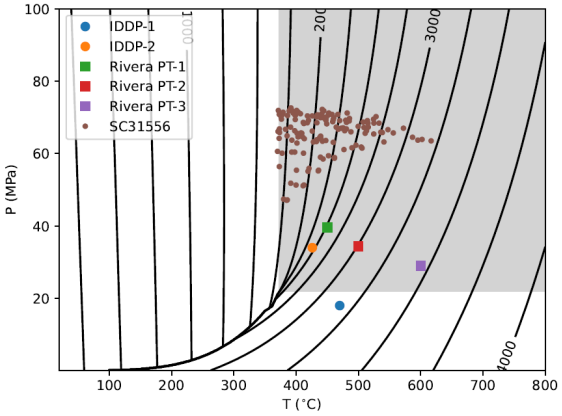

Figure 8: Pressures and temperature for blocks in the model with a temperature greater than 370°C.

Also shown in Figure 8 are the downhole PT conditions for IDDP-1 and IDDP-2 (Rivera and Burnell, 2023) and the bottom-hole PT conditions used by Rivera and co-workers

for simulations of the performance of wells feeding from supercritical conditions (Rivera, 2023; Rivera & Burnell, 2023; Rivera & Carey, 2023). Clearly, the supercritical zone in our model is deeper than that at IDDP-1 and IDDP-2, and the pressure gradient in our model is steeper than the hydrostatic conditions assumed by Rivera.

3. PRODUCTION/INJECTION SCENARIOS

3.1 Definition of scenarios

The scenarios investigated are listed in Table 2. They are partly based on those suggested by Gunnarsson et al. (2024).

Table 2: Production/Injection scenarios

No.	Name	Description
I	Base-case	Production and injection wells at standard depths
II	Deep production	Some production shifted down to the deep supercritical zone
III	Deep injection	Some injection shifted down to the deep supercritical zone
IV	Deep production & Injection	Both some production and some injection shifted down to the deep supercritical zone

The 12 production wells used in Scenario I are listed in Table 3 and the 8 injection wells are listed in Table 4. All the wells are operated on deliverability using the DELT option in AUTOUGH2. This option uses the same formula as the DELV option in TOUGH2 but sets a limit on the maximum mass flow. In the formulation of the DELV option, the mass flow of each phase (β=w for water and β=s for steam) is given by:

$$q_{m\beta} = \frac{k_{r\beta}}{\nu_\beta} \text{ PI } (P_\beta - P_{wb}) \qquad (1)$$

Table 3: Production wells used in Scenario I.

Well	Column	Layer	Elev. (mRL)	P (bar)	T (°C)	Max. flow kg/s
PRO02	avl	67	-2250	222	310	80
PRO06	aud	57	-550	81	265	50
PRO09	bbt	56	-450	74	266	40
PRO10	avk	62	-1100	125	265	80
PRO11	avu	62	-1100	125	280	80
PRO13	avn	55	-350	66	282	20
PRO14	azw	55	-350	66	271	50
PRO15	baq	55	-350	66	270	40
PRO16	avm	67	-2250	224	315	80
PRO17	bbw	62	-1100	127	311	80
PRO20	bbt	67	-2250	224	256	80
PRO21	avm	62	-1100	127	300	80

In (1), for each phase: $q_{m\beta}$ is the mass flow, $k_{r\beta}$ is the relative permeability, P_β is the pressure and ν_β is the kinematic viscosity, PI is the productivity index and P_{wb} is the flowing downhole pressure.

Initially, a moderate maximum mass flow was set at 80 kg/s for all wells, but it was found that some wells could not meet that target, so lower values were set (see Table 3). For all wells, a PI of 5.0E-12 was set and a flowing downhole pressure was estimated based on previous modelling experience. This will be improved in the future using supercritical wellbore simulations.

Table 4: Injection wells used in Scenario I.

Well	Column	Layer	Elevation	Type	Fraction
INJ01	bbr	52	-75	SGW[1]	0.21
INJ04	bck	52	-75	SGW	0.21
INJ07	aun	59	-750	SGW	0.21
INJ08	ayu	67	-2250	SGW	0.16
INJ22	axn	52	-75	SGW	0.21
INJ12	avq	52	-75	Con[2]	0.33
INJ19	azz	52	-75	Con	0.33
INJ18	bcx	52	-75	Con	0.34

1. SGW: separated geothermal water
2. Con: condensate

For Scenario II, the weak well PRO09 was replaced by a deep well, PRO30, which produced from the supercritical region in one of the faults. For Scenario III, the same production wells as Scenario I were used. However, the injection well INJ08 was replaced by a deep injector (INJ40) in the same column as the deep producer in Scenario II but with a feedzone one layer higher. Finally, in Scenario IV the deep producer PRO30 is used and a deep injector, INJ41, is located on the same fault but one layer above PRO30. Details of the deep wells discussed above are given in Table 5.

Table 5: Deep wells used in Scenarios II-IV.

Well	Column	Layer	Elev. (mRL)	P (bar)	T (°C)	Max. flow kg/s
PRO30	avm	77	-7250	611	476	80
INJ40	avm	76	-6750	585	443	16% of SGW
INJ41	aue	76	-6750	635	174	16% of SGW

ISSN 2703-4275

Figure 9 shows the locations of the production and injection wells superimposed on a plot of vertical permeability for the interior zone of the model showing the faults.

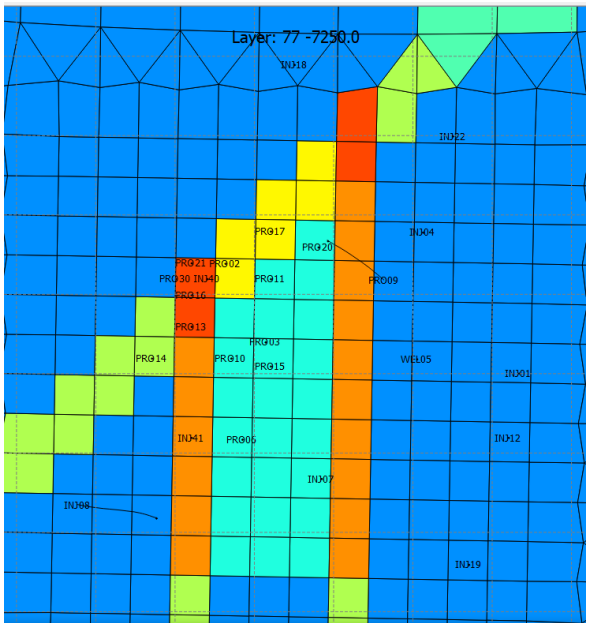

Figure 9: Location of wells. Also showing vertical permeability in layer 77.

The steam flow results for the four scenarios are shown in Figure 10. They show an obvious benefit of production from the supercritical region but only a very small benefit from deep reinjection. The results in Figure 10 probably understate the performance of the PRO30 as they are based on using the same separator pressure for all wells. PRO30 is likely to have a much higher wellhead pressure than the standard wells and to drive a turbine with a higher inlet pressure.

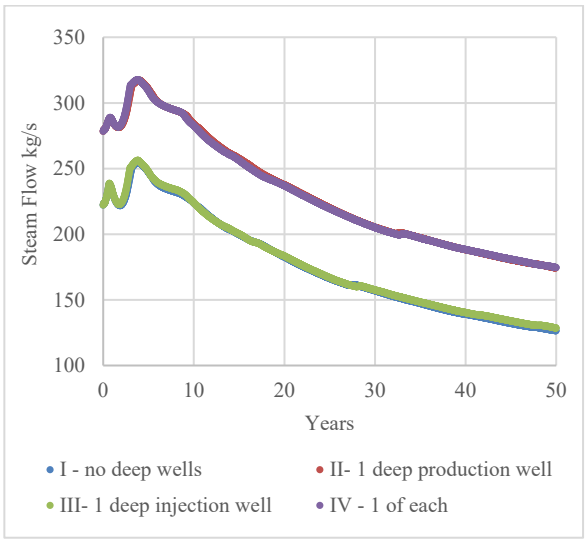

Figure 10: Steam flow for the four scenarios.

The performance of the supercritical production well, PRO30, in terms of enthalpy is shown in Figure 11. For both Scenario II and IV, the well sustains a production rate of 80 kg/s and as shown in Figure 11, there is very little effect produced by deep reinjection – just a very small reduction in enthalpy. Possibly a more aggressive production scenario should have been considered with the limit on mass production from PRO30 set greater than 80 kg/s.

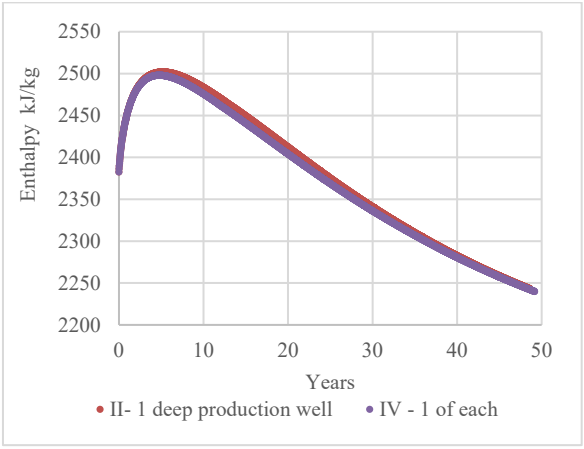

Figure 11: Enthalpy from the supercritical well, PRO30, for Scenarios II & IV.

4. CONCLUSION

Some preliminary numerical modelling results were reported for a whole-of-system model of a synthetic geothermal system based loosely on fields in the Taupo Volcanic Zone.

The natural state model shows a plausible convective upflow above a zone of high heat flow, centred at the intersection of faults.

The production model with wells drilled to standard depths gives a reasonable performance with total steam flow starting at 222 kg/s, rising to a peak of 254 kg/s after about 4 years, as the shallow steam zone expands, and then slowly declining to 126 kg/s after 50 years. A deep supercritical well, PRO30, boosts the steam production by 50-60 kg/s throughout the simulation period of 50 years.

Deep reinjection into the supercritical region has very little effect on production with or without a deep supercritical production well for the case study presented.

More work is required to determine better deliverability parameters for the production wells used in the simulation, particularly the supercritical well.

The study has shown that the modelling framework presented is an effective and appropriate tool for evaluating production and injection into supercritical zones of geothermal systems.

REFERENCES

Afanasyev, A.: Numerical modelling of brittle–ductile transition with the MUFITS simulator. Computational Geosciences, 24, 1651–1662. (2020)

Andersen, C., Weis, P.: Heat transfer from convecting magma reservoirs to hydrothermal fluid flow systems constrained by coupled numerical modeling. *Geophysical Research Letters*, *47*, e2020GL089463. (2020).

Asanuma, H., Mogi, T., Tsuchiya, N., Watanabe, N., Naganawa, S., Ogawa, Y., Fujimitsu, Y., Kajiwara,

T., Osato, K., Shimada, K., Horimoto, S., Sato, T., Yamada, S., Watanabe, K., Gotoh, Y.: Status of Japanese Supercritical Geothermal Project in FY2018, *GRC Transactions*, 43. (2019).

Asanuma, H., Mogi, T., Tsuchiya, N., Watanabe, N., Naganawa, S., Ogawa, Y., Fujimitsu, Y., Kajiwara, T., Osato, K., Shimada, K., Horimoto, S., Sato, T., Yamada, S. Watanabe, K.: Japanese supercritical geothermal project for drastic increase of geothermal power generation in 2050, *Proc. WGC 2020+1*, Reykjavik, Iceland. (2021).

Barton, S., O'Sullivan, J.P.: A Combined Regional Conceptual and Supercritical Numerical Model of the Reykjanes Peninsula. *Proc. World Geothermal Congress 2020+1,* Reykjavik, Iceland. (2021).

Battistelli, A., Finsterle, S., Pan, L.: Modeling of coupled wellbore-reservoir flow for supercritical geothermal systems in steam-like conditions. *Proc. TOUGH Symposium 2018*. Berkeley, California, USA. (2018).

Battistelli, A., Finsterle, S., Marcolini, M., Pan, L.: Modeling of coupled wellbore-reservoir flow for supercritical geothermal systems in steam-like conditions. Geothermics, 86, 101793. (2020).

Brikowski, T.H.: Modelling supercritical systems with TOUGH2: preliminary results using the EOS1sc equation of state module. *Proc. 26th Workshop on Geothermal Reservoir Engineering*, Stanford University, Stanford, California, USA. (2001).

Carey, B., Climo, M., Chambefort, I., Miller, C., Rae, A., Kissick, D., Bixley, P. & Winmill, R.: New Zealand's pathway to supercritical geothermal energy use: moving forward to exploration drilling, *Proc. 43rd New Zealand Geothermal Workshop*, Wellington, New Zealand. (2021)

Carson, B.: *Investigation of the Rotokawa Geothermal System and Feasibility of Supercritical Fluid Production within the TVZ through Supercritical TOUGH2 Numerical Modeling*, Masters Thesis, University of Victoria, Wellington, New Zealand. (2018).

Cladouhos, T., Callahan, O.: Heat extraction from superhot rock - technology development. *Proc. 49th Workshop on Geothermal Reservoir Engineering*, Stanford University, Stanford, California, USA. (2024).

Climo, M., Carey, B., Chambefort, I., Bendall, S., Blair, A.: Developing a strategy to accelerate utilisation of New Zealand's supercritical geothermal resources, *GRC Transactions*, 44. (2020).

Croucher, A.E. & O'Sullivan, M.J.: Application of the computer code TOUGH2 to the simulation of supercritical conditions in geothermal systems, *Geothermics*, 37, 622-634. (2008).

Dobson, P., Asanuma, H., Huenges, E., Polleto, F., Reinsch, T., Sanjuan, B.: Supercritical geothermal systems - a review of past studies and ongoing research activities. *Proc. 41st Workshop on Geothermal Reservoir Engineering*, Stanford University, Stanford, California, USA. (2017).

Driesner, T.: Supercritical and Superhot Geothermal Resources - Some Fundamental Insights, *Proc. WGC 2020+1*, Reykjavik, Iceland. (2021).

Elders, W., Friedliefsson, G., Albertsson, A.: Drilling into magma and the implications of the Iceland Deep Drilling Project (IDDP) for high-temperature geothermal systems worldwide. *Geothermics*, 49, 111–118. (2014).

Ellis, S.E., Little, T.A., Wallace, L.M., Hacker, B.R., Buiter, S.J.H.: Feedback between rifting and diapirism can exhume ultrahigh-pressure rocks. *Earth Plan. Sci. Let.*, 311, 427-438. (2011).

Ellis, S., Kissling, W., Rae, A., Villamor, P.: Toward magmatic source models for Ngakuru Graben, Taupo Rift, New Zealand. *Proc. 37th New Zealand Geothermal Workshop,* Taupo*,* New Zealand. (2015).

Feng, G., Xu, T., Wang, F., Wang, Y. Jiang. Z.: Modeling analyses of fluid flow and reactive transport processes for a supercritical geothermal system, *Proc. WGC 2020+1*, Reykjavik, Iceland. (2021a).

Feng, G., Wang, Y., Xu, T., Wang, F. & Yan Shi, Y.: Multiphase flow modeling and energy extraction performance for supercritical geothermal systems, *Renewable Energy*, 173, 442-454. (2021b).

Fridleifsson, G.O.: IDDP-2 - drilling into the supercritical at Reykjanes, *Proc. 39th New Zealand Geothermal Workshop*, Rotorua, New Zealand. (2017).

Hayba, D.O., Ingebritsen, S.E.: The Computer Model HYDROTHERM, a Three-Dimensional Finite-Difference Model to Simulate Ground-Water Flow and Heat Transport in the Temperature Range of 0-1200°C, U.S. Geological Survey Water Resources Investigation 94-4045, Reston, VA (1994).

Hayba, D.O., Ingebritsen, S.E.: Multiphase Groundwater Flow near Cooling Plutons, *J. Geophys. Res.*, 102, 12,235-12,252. (1997).

Hermanska, M., Stefansson, A., Scott, S.: Supercritical fluids around magmatic intrusions: IDDP-1 at Krafla, Iceland. *Geothermics*, 78, 101–110. (2019).

Ishitsuka, K., Kobayashi, Y., Watanabe, N., Yamaya, Y., Bjarkason, E., Suzuki, A., Mogi, T., Asanuma, H., Kajiwara, T., Sugimoto, T., Saito, R.: Bayesian and neural network approaches to estimate deep temperature distribution for assessing a supercritical geothermal system: evaluation using a numerical model, *Natural Resources Research*, 30 (5). (2021).

Kissling, W.M.: Extending MULKOM to supercritical temperatures and pressures, *Proc. WGC 1995*, Florence, Italy, 1687-1690. (1995).

Kissling, W.: Large scale numerical models of TVZ-type geothermal fields. *Proc. 18th New Zealand Geothermal Workshop*, Auckland, New Zealand. 275-280. (1996).

ISSN 2703-4275

Kissling, W.M.: Large Scale Hot Plate Models for the TVZ Geothermal Fields. *Proc. 19th New Zealand Geothermal Workshop,* Auckland, New Zealand. 51-56. (1997).

Kissling, W.M.: Source models for the TVZ geothermal fields. *Proc. 20th New Zealand Geothermal Workshop,* Auckland, New Zealand. 147-152. (1998).

Kissling, W.M.: Modeling of cooling plutons in the Taupo Volcanic Zone, New Zealand. *Proc. 24th Workshop on Geothermal Reservoir Engineering*, Stanford University, Stanford, California, USA. (1999).

Kissling, W., Ellis, S., Charpentier, F., Bibby, H.: Convective flows in a TVZ-like setting with a brittle-ductile transition. Transport in Porous Media, 77, 335-355. (2009).

Kissling, W., Ellis, S., Charpentier, F., Bibby, H.: Large scale convective flows with a brittle-ductile transition. *Proc*. *World Geothermal Congress 2010***,** Bali, Indonesia. (2010).

Kissling, W.M and Ellis, S.E.: Modelling the flow of hydrothermal fluids above an evolving continental rift. *Proc. 33rd New Zealand Geothermal Workshop,* Auckland*,* New Zealand. (2011).

Kissling, W.M and Ellis, S.E.: Modelling deep production and injection using a regional scale model of a TVZ-like geothermal field. *Proc. 34th New Zealand Geothermal Workshop,* Auckland*,* New Zealand. (2012).

Kissling, W.: A testbed for a new generation geothermal simulator. *Proc. 36th NZ Geothermal Workshop*, Auckland, New Zealand. (2014).

Kissling, W., Ellis, S., Barker, S., Caldwell, T.: A source-to-surface model of heat and fluid transport in the Taupo Rift, New Zealand. *Journal of Volcanology and Geothermal Research,* 446, 107995. (2024).

Lamy-Chappuis, B., Yapparova, A. Driesner, T.: An advanced well and reservoir model for supercritical and saline geothermalapplications, the example of IDDP-2, *Proc. WGC 2020+1*, Reykjavik, Iceland. (2021).

Lamy-Chappuis, B., Yapparova, A. & Driesner, T.: Simulations of the IDDP-2 well, Reykjanes, Iceland, and its behavior in different operation scenarios, *Geothermics*, 114, 102790. (2023).

Magnusdottir, L.: Modeling the deep roots of geothermal systems. *Proc. 39th Workshop on Geothermal Reservoir Engineering*, Stanford University, Stanford, California, USA. (2014).

Magnusdottir, L., Finsterle, S.: An iTOUGH2 equation-of-state module for modeling supercritical conditions in geothermal reservoirs, *Geothermics*, 57, 8–17. (2015). doi:10.1016/j.geothermics.2015.05.003.

Magnusdottir, L., Jonsson, M.T.: Increased reliability of supercritical EOS1sc module in iTOUGH2, *Proc. 43rd Workshop on Geothermal Reservoir Engineering*, Stanford University, Stanford, California, USA. (2018).

Oka, D., Tamura, M., Mogi, T., Nakagawa, M., Takahashi, H., Ohzono, M., Ichiyanagi, M.: Conceptual model of supercritical geothermal system in Shiribeshi Region, Hokkaido, Japan. *Geothermics*, 108, 102617. (2023).

O'Sullivan, J.P., O'Sullivan, M.J., Croucher, A.: Improvements to the AUTOUGH2 supercritical simulator with extension to the air-water equation-of-state, *GRC Transactions,* 40, 921-929. (2016).

O'Sullivan, J., Newson, J., Alcaraz, S., Barton, S., Baraza, R., Croucher, A., & O'Sullivan, M. (2020). A Robust supercritical geothermal simulator. *Proc. 42nd New Zealand Geothermal Workshop*. Waitangi, New Zealand.

Parisio, F., Vilarrasa, V., Wang, W., Kolditz, O., Nagel, T.: The risks of long-term re-injection in supercritical geothermal systems. *Nature Communications*, 10:4391. (2019).

Pashkevich, R. & Taskin, V.: Numerical simulation of exploitation of supercritical enhanced geothermal system. *Proc*. *World Geothermal Congress 2010***,** Bali, Indonesia. (2010).

Pritchett, J.W.: STAR: A Geothermal Reservoir Simulation System, *Proc. World Geothermal Congress 1995*, Florence, Italy. (1995).

Pruess, K., Oldenburg, C., Moridis, G.: *TOUGH2 User's Guide Version 2.0*, Report LBNL-43134, Earth Sciences Division, Lawrence Berkeley National Laboratory, University of California, Berkeley, CA 94720, USA. 210 p. (1999).

Raguenel, M., Driesner, T., Bonneau, F.: Numerical modeling of the geothermal hydrology of the Volcanic Island of Basse-Terre, Guadeloupe. *Geothermal Energy*, 7, 28. (2019).

Reinsch, T., Dobson, P., Asanuma, H., Huenges, E., Poletto, F., Sanjuan, B.: Utilizing supercritical geothermal systems: a review of past ventures and ongoing research activities. *Geothermal Energy*, 5, 16. (2017).

Rendel, P.M., Mountain, B.W., Sajkowski, L. & Chambefort, I.: Experimental studies of supercritical fluid-rock interactions - geothermal: the next generation, *Proc. 43rd New Zealand Geothermal Workshop*, Wellington, New Zealand. (2021)

Renaud, T., Popineau, J., Riffault, J., O'Sullivan, J., Gravatt, M., Yeh, A., Croucher, A., O'Sullivan, M.: Practical workflow for training in geothermal reservoir modelling. *Proc. 43rd New Zealand Geothermal Workshop*. Wellington, New Zealand. (2021).

Rivera, J. (2023). Comparison of Icelandic Supercritical Well Forecasts with Subcritical Geothermal Production Well Outputs. *Proc. 45th New Zealand Geothermal Workshop*, Auckland, New Zealand.

Rivera, J. & Burnell, J. (2023). Supercritical Well Performance Simulation using GFlow Wellbore Simulator: A Case Study of Ultra-hot IDDP Wells in Iceland. *Proc. 45th New Zealand Geothermal Workshop*, Auckland, New Zealand.

Rivera, J. & Carey, B. (2023). Comparative geothermal well performance – supercritical and subcritical. GNS Science Report: 2023/01. GNS Science, Lower Hutt, New Zealand,

Sato, T., Osato, K., Kissling, W.M., White, S. P., Takahashi, Y., Ito, M., Koide, K.: A study of production from a super critical deep seated geothermal reservoir using TOUGH2 numerical simulation, *Proc. 21st New Zealand Geothermal Workshop,* Auckland, New Zealand. (2000).

Sato, T., Ohsato, K., Shiga, T., Sato, M., White, S. P., Kissling, W.M.: A study of reservoir estimation for a deep-seated geothermal reservoir using TOUGH2 and CHEMTOUGH2. *Proc. TOUGH Symposium 2003*, Lawrence Berkeley National Laboratory, Berkeley, California, USA. (2003).

Scott, S., Driesner, T., Weis, P.: Geologic controls on supercritical geothermal resources above magmatic intrusions. Nature Communications, 6. (2015a).

Scott, S., Driesner, T., Weis, P.: Hydrology of a supercritical flow zone near a magmatic intrusion in the IDDP-1 well—insights from numerical modeling. In: Proceedings, World Geothermal Congress 2015, Melbourne, Australia. (2015b).

Scott, S., Driesner, T., Weis, P.: The thermal structure and temporal evolution of high-enthalpy geothermal systems. *Geothermics*, 62, 33–47. (2016).

Scott, S.: The hydrology of 'superhot' and 'supercritical' geothermal resources in magma-driven geothermal systems, *GRC Transactions*, 42. (2018).

Scott, S., O'Sullivan, J.P., Maclaren, O., Nicholson, R., Covell, C., Newson, J., Gudjonsdottir, M.: Bayesian calibration of a natural state geothermal reservoir model, Krafla, North Iceland. *Water Resources Research*, *58*, e2021WR031254. (2022).

Scott, S., Yapparova, A., Weis, P., Houde, M.: Hydrological constraints on the potential of enhanced geothermal systems in the ductile crust. Geothermal Energy, 12, 10. (2024).

Stimac, J., Wilmarth, M., Mandeno, P.E., Dobson, P., Winick, J.: Review of exploitable supercritical geothermal resources to 5 km at Geysers-Clear Lake, Salton Sea, and Coso, *GRC Transactions*, 41. (2017).

Sudarmadi, E., Zarrouk, S., Croucher, A., Bramantyo, E.A.: Modelling production from supercritical geothermal reservoirs. *Proc. 34th New Zealand Geothermal Workshop,* Auckland*,* New Zealand. (2012).

Suzuki, Y., Akatsuka, T., Yamaya, Y., Watanabe, N., Okamoto, K., Osato, K., Kajiwara, T., Ogawa, Y., Mogi, T., Tsuchiya, N., Asanuma, H.: Estimation of an ultra-high-temperature geothermal reservoir model in the Kakkonda geothermal field, northeastern Japan, *Geothermics*, 105, 102525. (2022).

Tsuchiya, N.: Potential Candidates of Supercritical Geothermal Reservoir, *GRC Transactions*, 41. (2017).

Wagner, W., Cooper, J.R., Dittman, A., Kijima, J., Kretzschmar, H.-J., Kruse, A., Mareš, R., Oguchi, K., Sato, H., Stöcker, I., Šifner, O., Takaishi, Y., Tanishita, I., Trübenbach, J., Willkommen, Th.: The IAPWS Industrial Formulation 1997 for the Thermodynamic Properties of Water and Steam, *ASME J. Eng. Gas Turbines and Power*, 122, 150-182. (2000).

Wang, Y., Xu, T., Cheng, Y., Feng, G.: Prospects for power generation of the doublet supercritical geothermal system in Reykjanes Geothermal Field, Iceland, *Energies*, 15, 8466. (2022).

Watanabe, K., Niibori, Y., Hashida, T.: Numerical study on heat extraction from a supercritical geothermal reservoir, *Proc.* World Geothermal Congress 2000, 3957-3961. (2000).

Weis, P., Driesner, T., Coumou, D., Geiger, S.: Hydrothermal, multiphase convection of H2O-NaCl fluids from ambient to magmatic temperatures: a new numerical scheme and benchmarks for code comparison. Geofluids, 14, 347–371, (2014).

Xu, T., Feng, G., Wang, Y.: Numerical modeling on fluid dynamics and phase changes for a supercritical geothermal system. *Proc. 45th Workshop on Geothermal Reservoir Engineering*, Stanford University, Stanford, California, USA. (2020).

Xu, T., Feng, G., Gong, Y.: An improved reactive transport model for supercritical geothermal systems. *Proc. 48th Workshop on Geothermal Reservoir Engineering*, Stanford University, Stanford, California, USA. (2023).

Yano, Y., Ishido, T.: Numerical investigation of production behavior of deep geothermal reservoirs at supercritical conditions, *Geothermics*, **27**, 705–721. (1998).

ISSN 2703-4275